



## Results

### The $\beta_1$ AR and $\beta_2$ AR binding sites

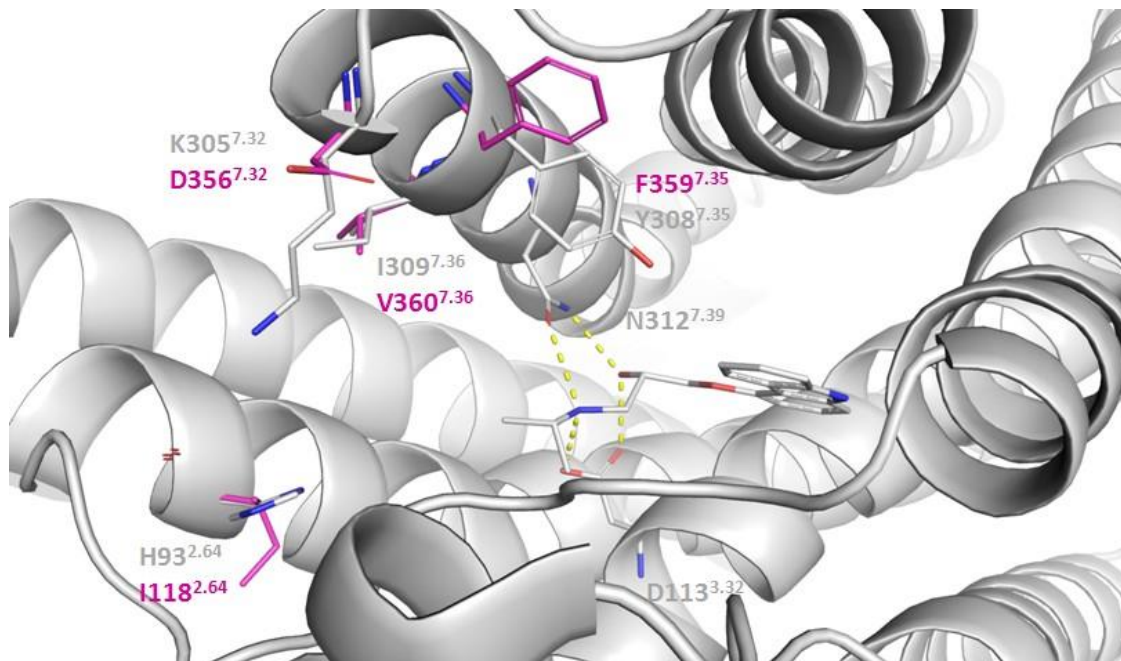


Figure S1: Comparison of the human  $\beta_1$ AR (residues in magenta, model downloaded from the GPCRdb) and the human  $\beta_2$ AR (residues in light grey, PDB code: 2RH1) binding sites. Carazolol, which is bound to the  $\beta_2$ AR structure, is shown with white sticks.

## Pharmacological analysis of the 21 core fragments

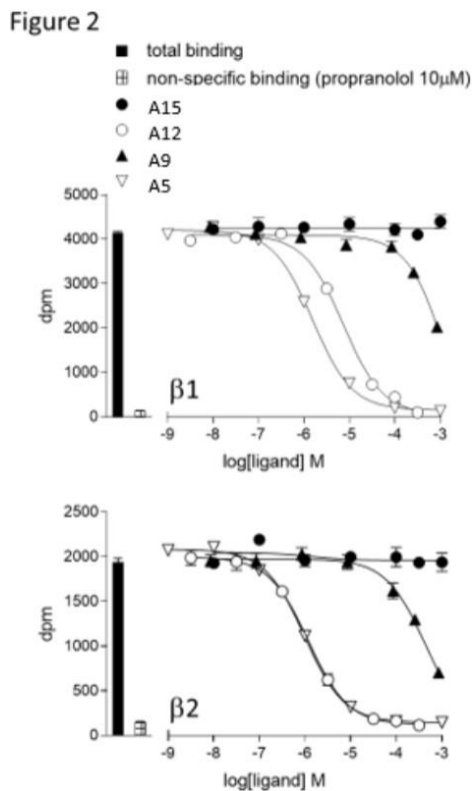


Figure S2: Inhibition of  $^3\text{H}$ -CGP12177 binding to CHO- $\beta_1$  and CHO- $\beta_2$  cells by core compounds **A5**, **A9**, **A12** and **A15**. Bars represent total  $^3\text{H}$ -CGP12177 binding and non-specific binding (determined in the presence of 10  $\mu\text{M}$  propranolol). The concentration of  $^3\text{H}$ -CGP12177 was 0.94 nM. Data points are mean  $\pm$  s.e.m. of triplicate determinations.

Table S1: Affinity (log  $K_D$  values) of core compounds 1-21 obtained from  $^3\text{H}$ -CGP 12177 whole cell binding in CHO cells stably expressing the human  $\beta_1\text{AR}$  or  $\beta_2\text{AR}$ . Values represent mean  $\pm$  or - s.e. mean of n separate experiments. Selectivity ratios are also given where a ratio of 1 demonstrates no selectivity for a given receptor subtype over another. When the competing ligand caused  $> 50\%$  inhibition of specific binding, an  $\text{IC}_{50}$  value was determined by extrapolating the curve to non-specific levels and assuming that a greater concentration would have resulted in 100% inhibition. These values are given as apparent  $K_D$  values in the data table.

Article ID	$\beta_1\text{AR}$ Log $K_D$	n	$\beta_2\text{AR}$ Log $K_D$	n	Selectivity ratio
A1	$-5.44 \pm 0.03$	11	$-5.62 \pm 0.02$	11	1.5
A2	$-5.49 \pm 0.04$	10	$-5.59 \pm 0.04$	10	1.3
A3	$-5.62 \pm 0.02$	10	$-5.93 \pm 0.03$	10	2.0
A4	$-6.77 \pm 0.03$	12	$-7.45 \pm 0.04$	12	4.8
A5	$-6.39 \pm 0.03$	10	$-6.87 \pm 0.04$	9	3
A6	No binding	6	No binding	6	
A7	No binding	6	No binding	6	
A8	$-4.01 \pm 0.03$ apparent	6	$-4.78 \pm 0.02$	6	5.9
A9	$-3.71 \pm 0.05$ apparent	5	$-4.34 \pm 0.05$ apparent	6	4.3
A10	$-3.98 \pm 0.03$ apparent	6	$-4.48 \pm 0.03$ apparent	6	3.2
A11	$-4.70 \pm 0.05$	6	$-5.69 \pm 0.03$	6	9.8
A12	$-5.70 \pm 0.05$	6	$-6.67 \pm 0.05$	6	9.3
A13	$-4.26 \pm 0.04$ apparent	6	$-4.64 \pm 0.05$ apparent	6	2.4
A14	$-4.15 \pm 0.03$ apparent	6	$-4.84 \pm 0.04$	6	4.9
A15	No binding	6	No binding	6	
A16	$-3.71 \pm 0.02$ apparent	5	$-4.23 \pm 0.05$ apparent	6	3.3
A17	$-4.24 \pm 0.04$ apparent	6	$-4.73 \pm 0.03$ apparent	6	3.1
A18	No binding	6	No binding	6	
A19	$-4.22 \pm 0.02$ apparent	6	$-4.63 \pm 0.03$ apparent	6	2.6
A20	$-3.73 \pm 0.04$ apparent	6	$-4.38 \pm 0.05$ apparent	6	4.5
A21	No binding	6	No binding	6	

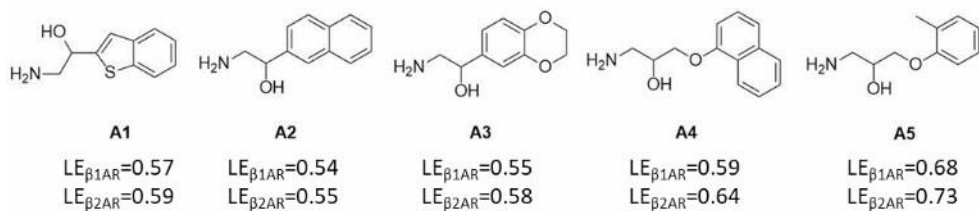


Figure S3: The five core fragments selected for further growing.

## Library synthesis

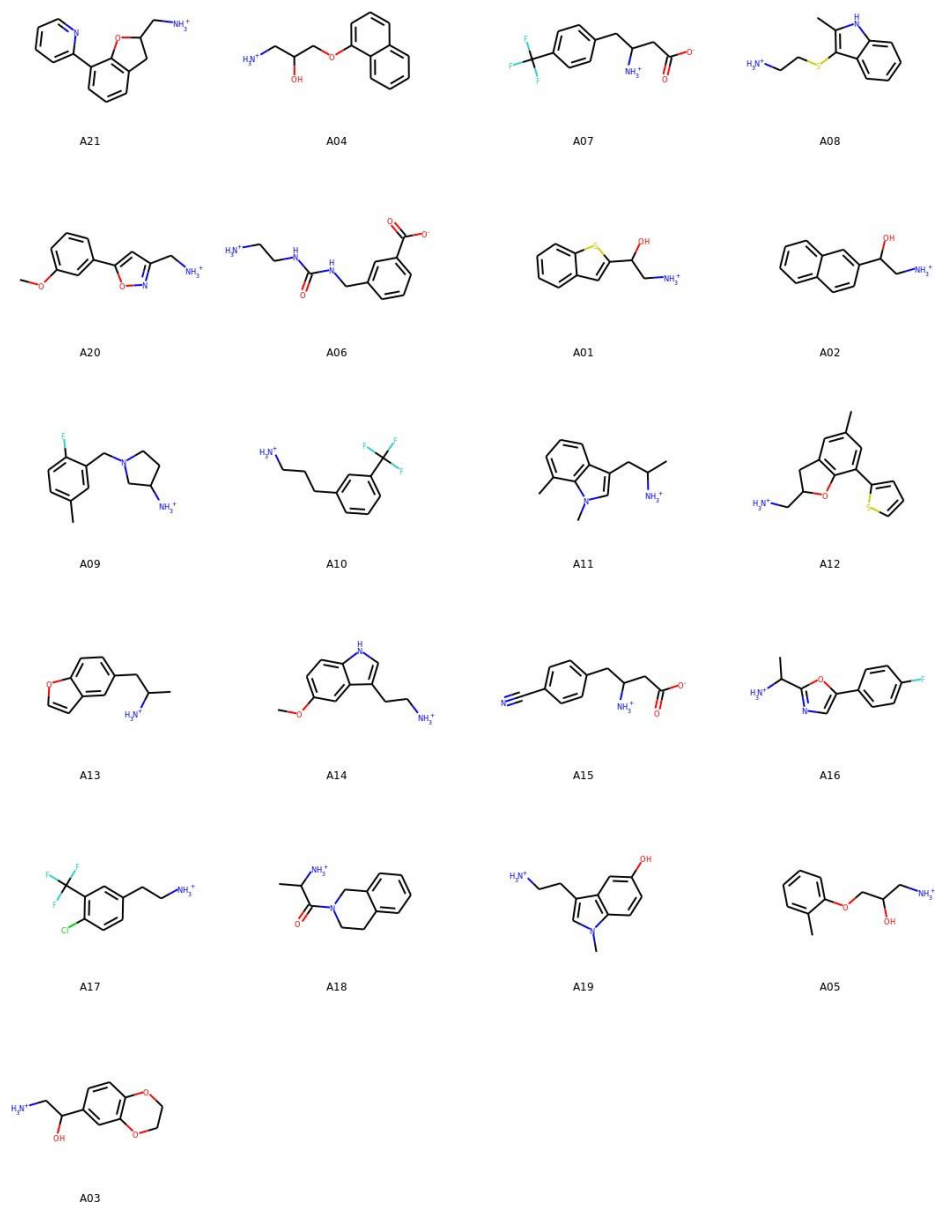


Figure S4: 2D depiction of the 21 OBP fragments.

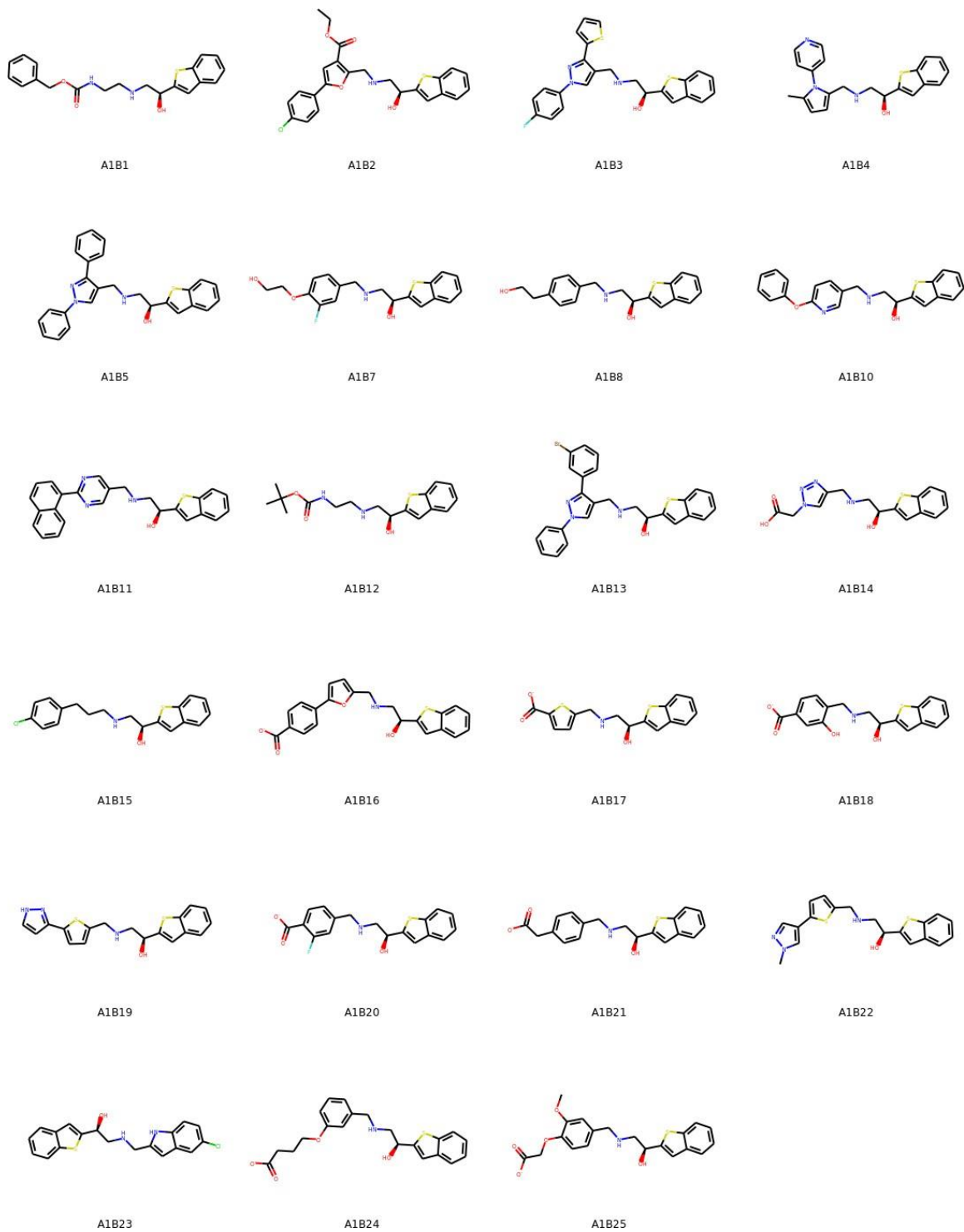


Figure S5: 2D depiction of the **A1** derivative products.

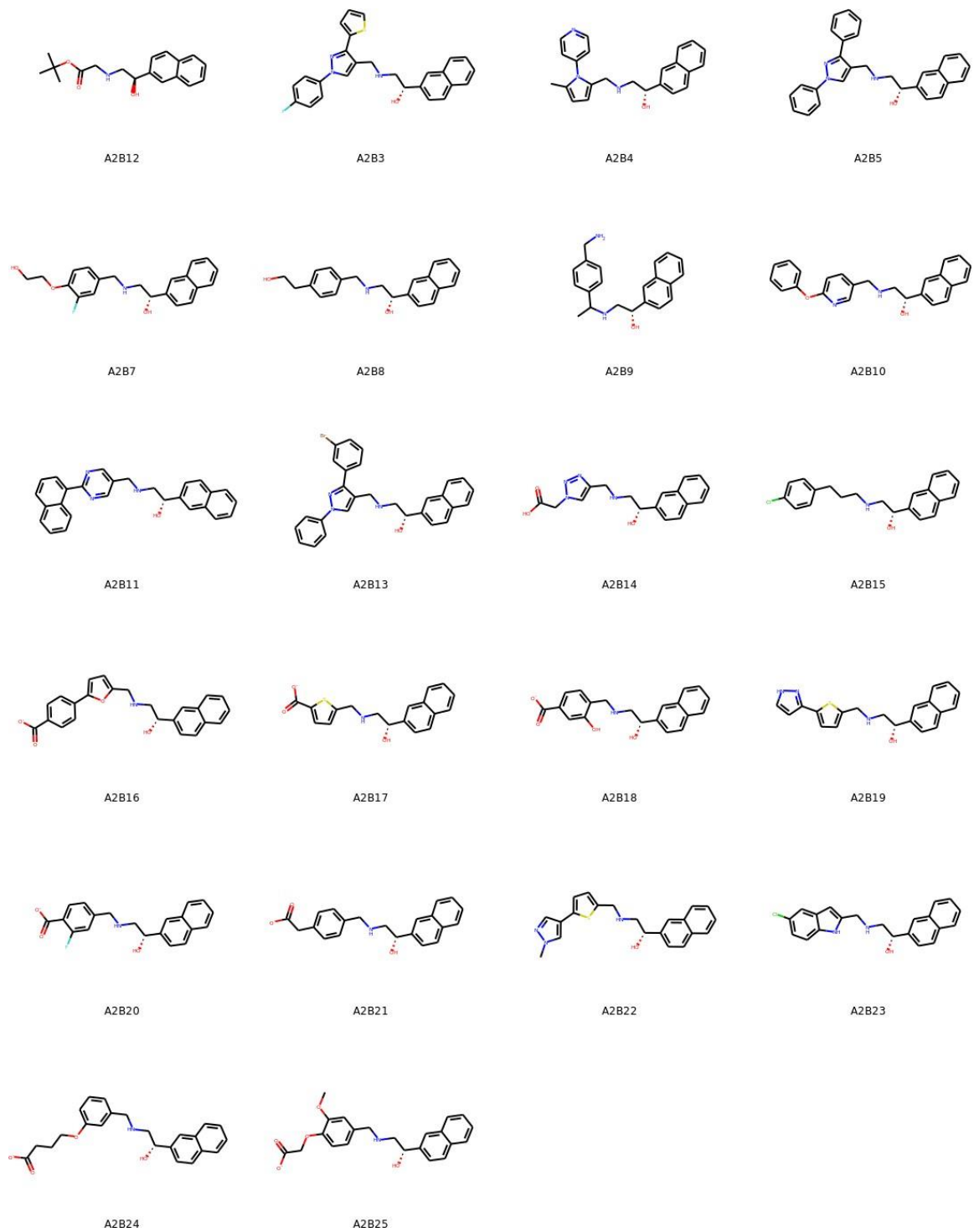


Figure S6: 2D depiction of the **A2** derivative products.

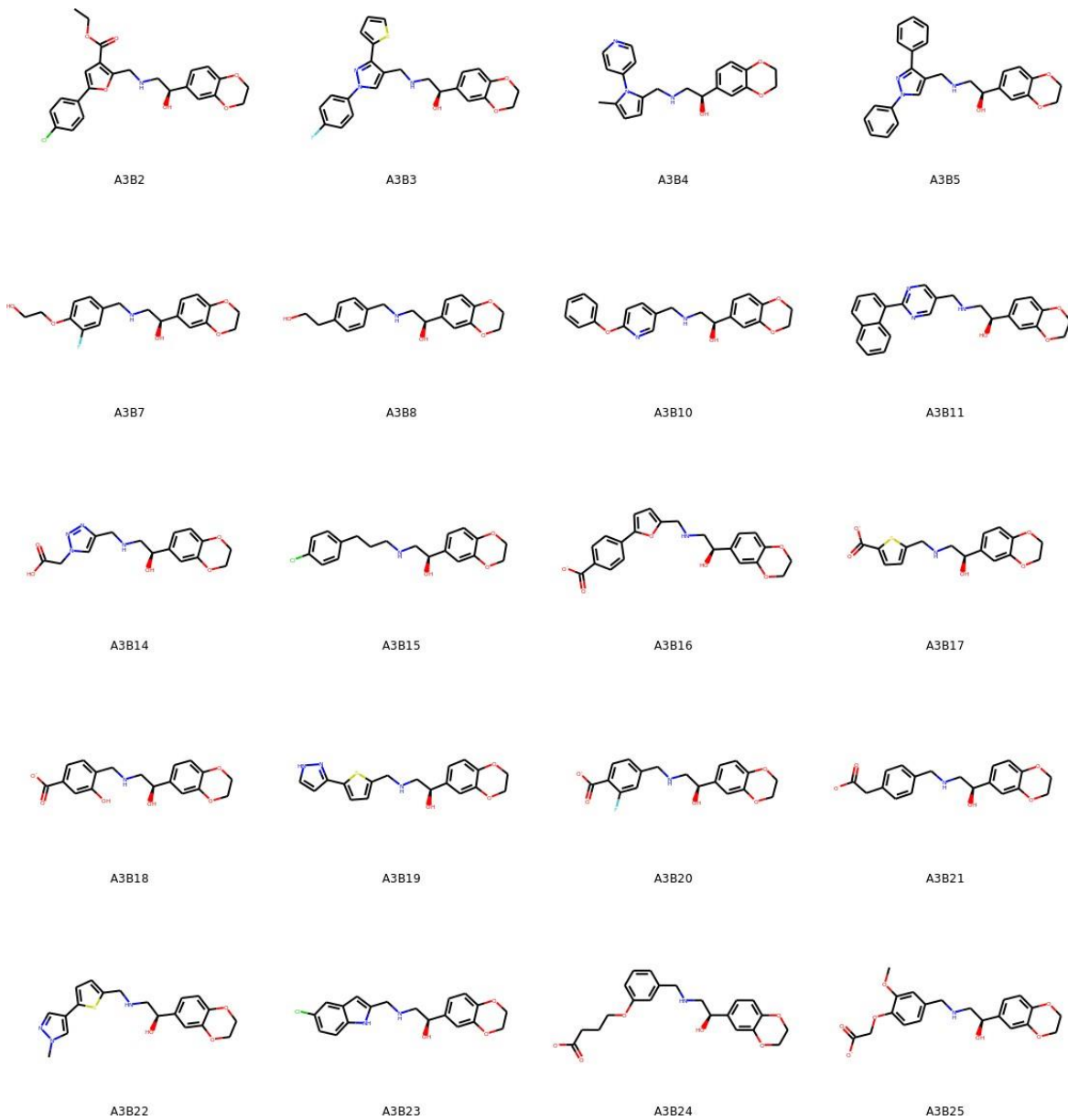


Figure S7: 2D depiction of the **A3** derivative products.

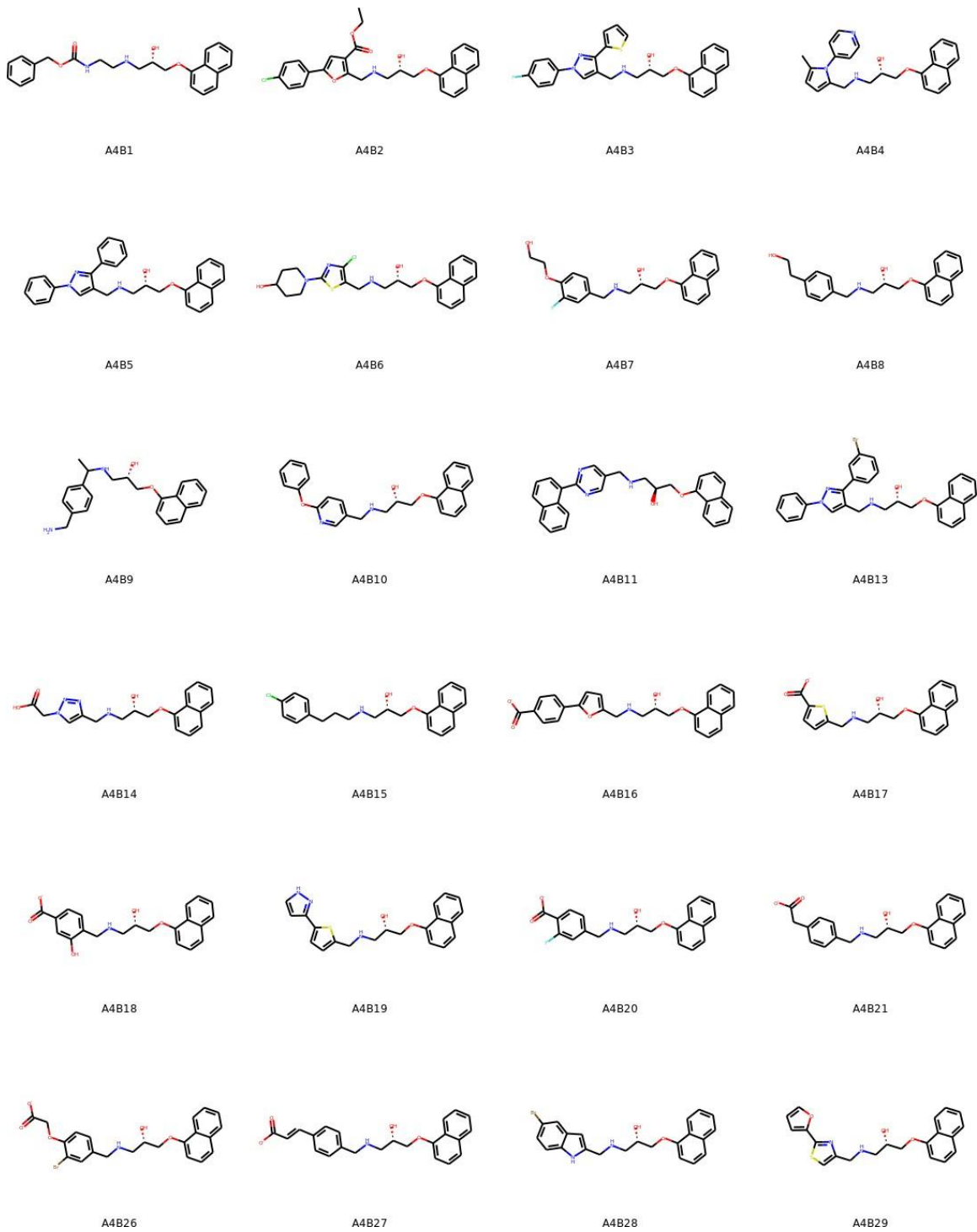


Figure S8: 2D depiction of the **A4** derivative products.

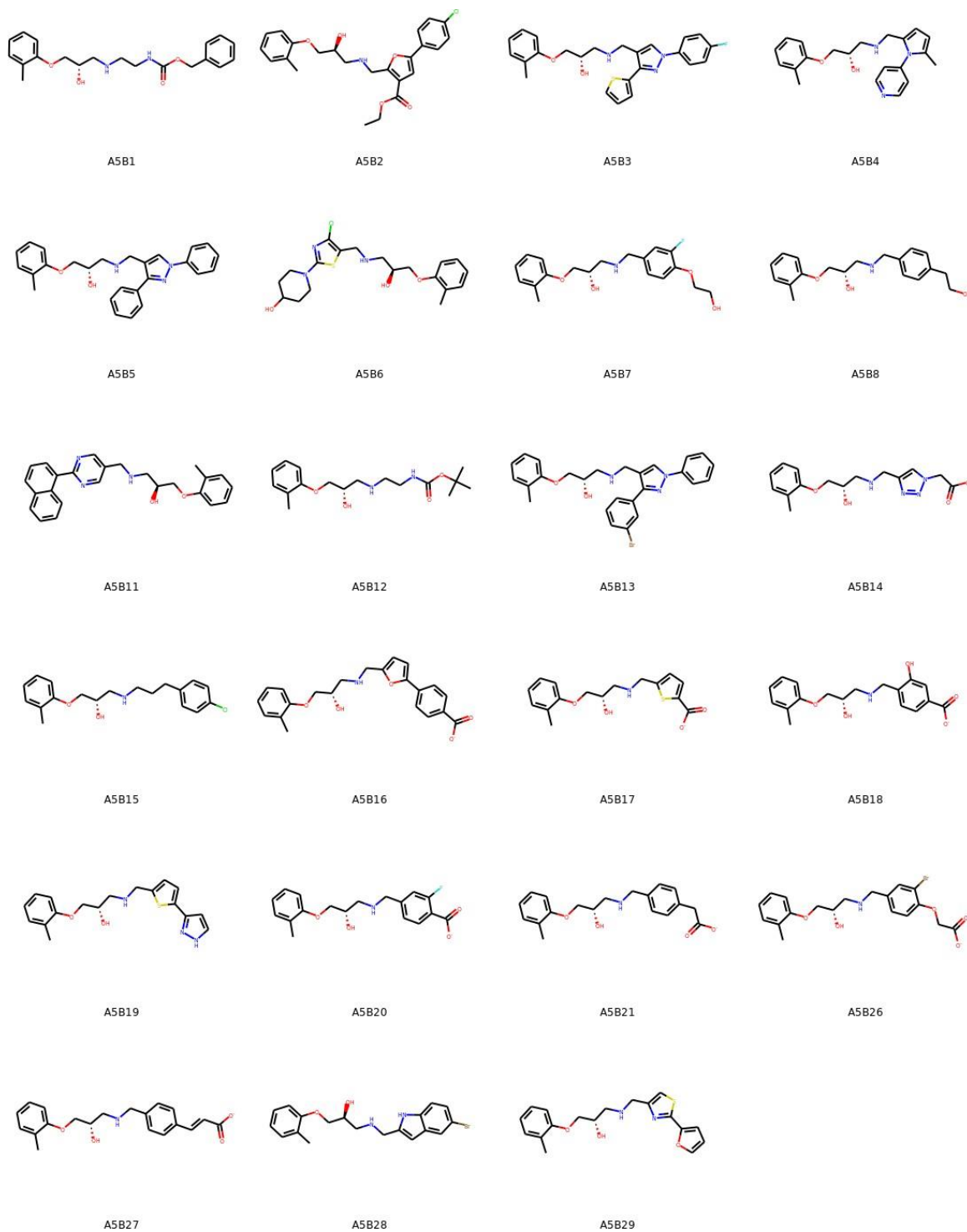


Figure S9: 2D depiction of the **A5** derivative products.

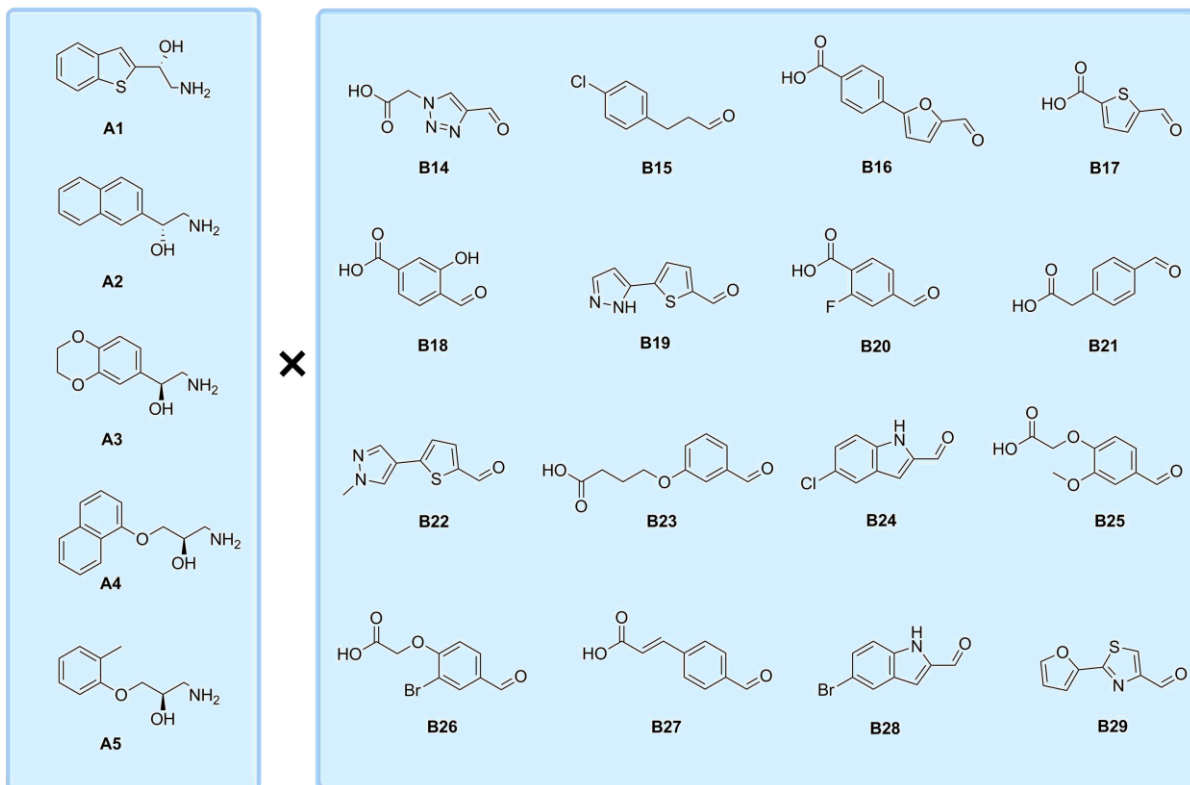


Figure S10: Matrix of the designed bitopic compounds for  $\beta_2$ AR.

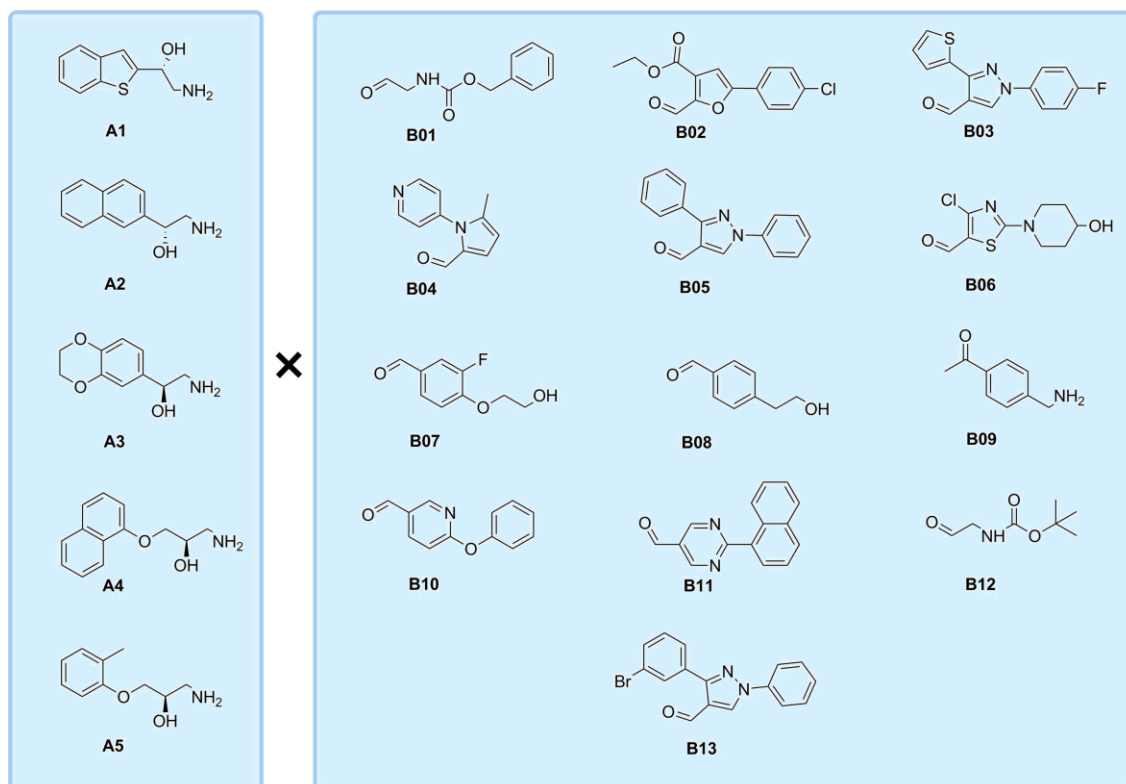


Figure S11: Matrix of the designed bitopic compounds for the  $\beta_1$ AR.

## Success rate of the library synthesis

	A1	A2	A3	A4	A5
B1		*	#	*	
B2		*		*	*
B3		*		*	
B4	*	*		*	
B5		*		*	#
B6	#	*	#	*	#
B7		*		*	
B8		*		*	
B9	*	*	#	*	#
B10		*			#
B11		*			
B12		*			
B13		*			
B14		*			
B15				*	
B16	#	*			
B17		*			
B18		*			
B19		*		*	
B20		*			
B21		*		*	
B22		#			
B23		*			
B24			#		
B25					
B26					
B27					
B28				*	
B29					

Figure S12: A. Success rate of the  $\beta_1$  matrix; \* 5 eq. AcOH added; # only dialkylated product formed. B. Success rate of the  $\beta_2$  matrix; \* 5 eq. AcOH added; # only dialkylated product formed, grey cells: not reacted in the sparse matrix.

## Pharmacological analysis of the optimization matrices

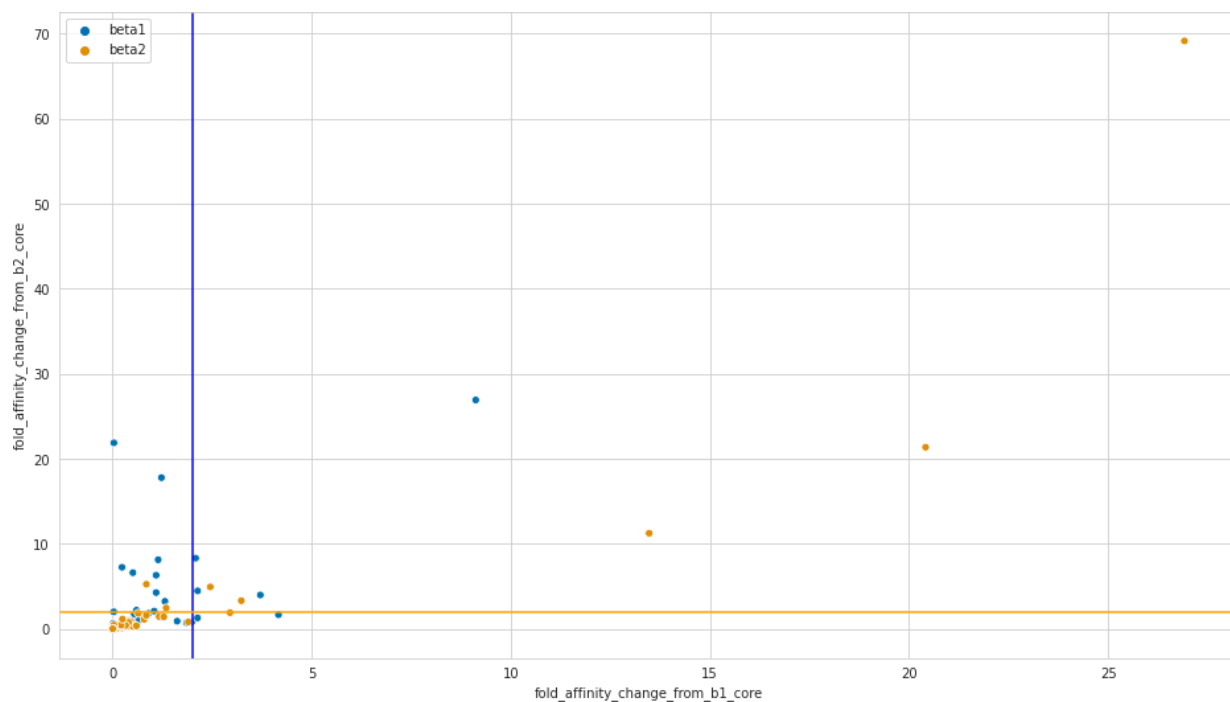
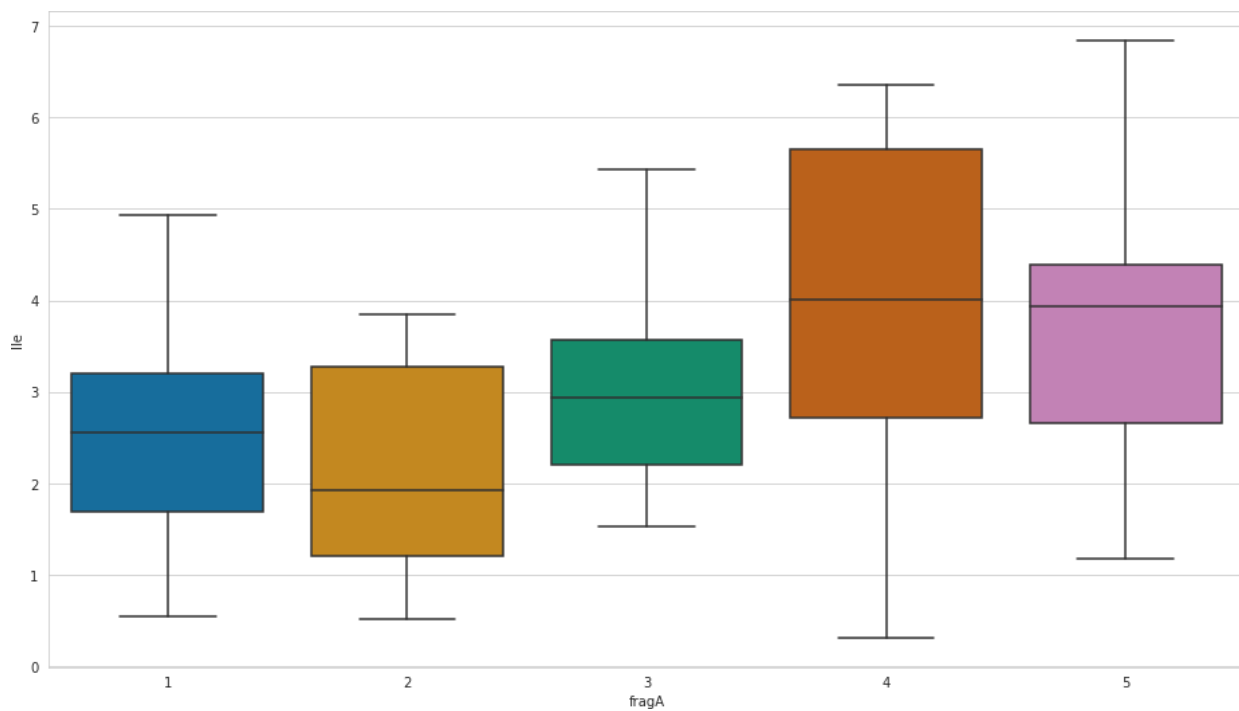
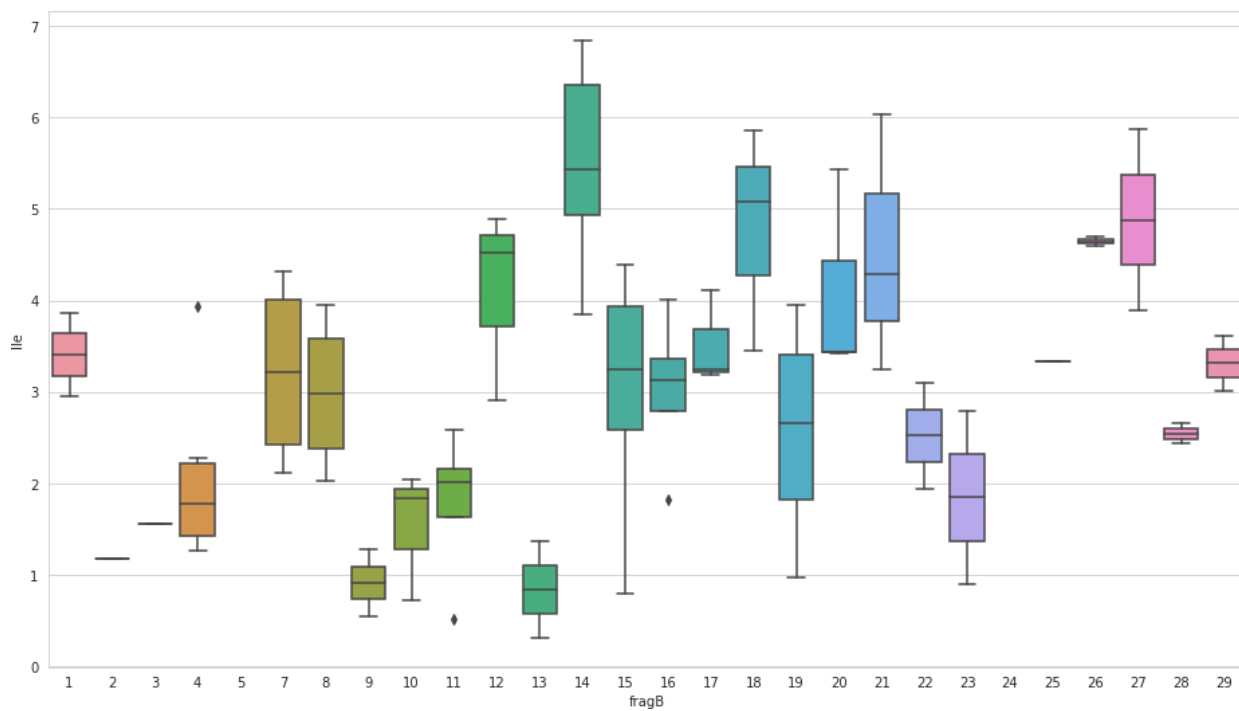


Figure S13: Scatter plot distribution of the affinity gain for the  $\beta_1$ -SBP bitopic compounds (blue dots) and the  $\beta_2$ -SBP bitopic compounds (orange dots) when compared to their initial OBP fragments. The vertical blue line separates the compounds which exhibit an improved affinity against the  $\beta_1$ AR versus the ones which do not. Thus any blue point (i.e. designed to bind to the  $\beta_1$ AR) located to the right of the blue line can be regarded as a positively designed compounds. The same logic applies for the  $\beta_2$ AR-SBP bitopic compounds and the horizontal orange line.



(a)



(b)

Figure S14: Box plot representation of the LLE of the (a) core OBP fragments and (b) theSBP fragments in both optimization matrices.

# Methods

## Chemical synthesis

All chemical reagents used were purchased from commercial chemical suppliers. Flash chromatography was performed using Teledyne ISCO CombiFlash Lumen+ Rf. Purifications by preparative-HPLC were performed with Hanbon NS4205 Binary high pressure semi-preparative HPLC.

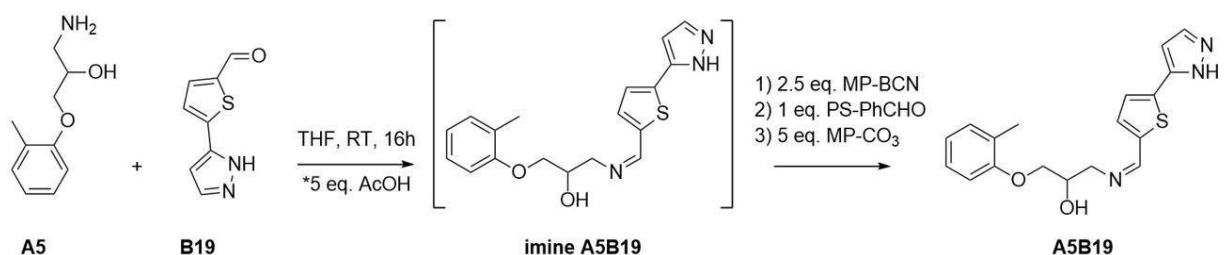


Figure S15: Example of a reductive alkylation. Primary amine (A5) and aromatic aldehyde(B19), the imine intermediate (imine A5B19) and secondary amine product A5B19.

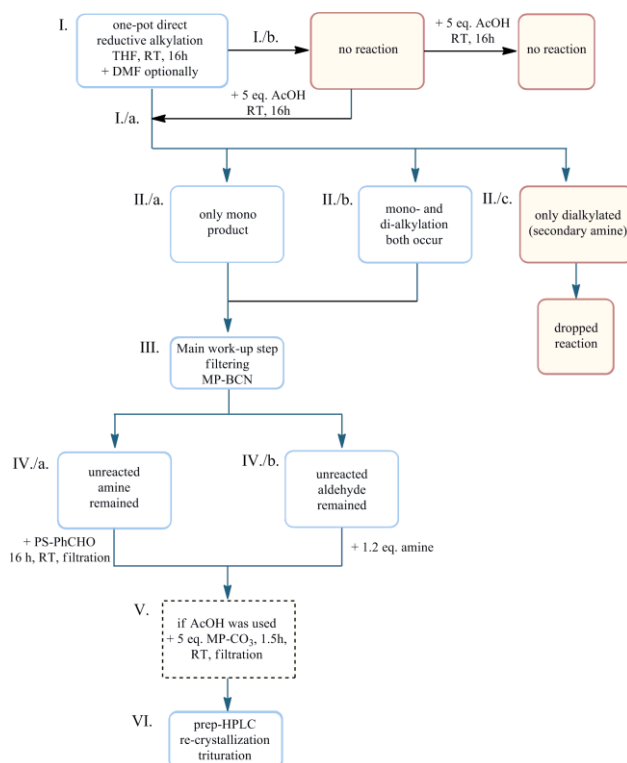


Figure S16: General procedure for reductive alkylation library synthesis.

## Characterisation of the library members

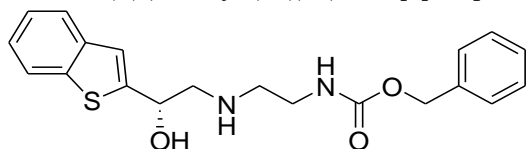
The LC-MS measurements were performed on Shimadzu LCMS2020 LC/MS system. The purity of all compounds was over 90% based on LC-MS measurements. High resolution mass spectrometric measurements were performed using a Q-TOF Premier mass spectrometer (Waters Corporation, Milford, MA, USA) in positive electrospray ionization mode. The NMR experiments were performed at 500 MHz ( $^1\text{H}$ ) on a Varian VNMR SYSTEM spectrometer. Chemical shifts are referenced to the residual solvent signals, 2.50 ppm for  $^1\text{H}$  in DMSO- $d_6$  and 7.28 ppm for  $^1\text{H}$  in  $\text{CDCl}_3$ .

### HR-MS results of the $\beta_1$ -receptor matrix

Compound	Mass (Da)	Calculated Mass (Da)	Measurement Error (ppm)	Formula	Measured Ion
A1B1	371.1416	371.1429	-3.5	C20H22N2O3S	M+H
A1B2	456.1030	456.1036	-1.3	C24H22ClNO4S	M+H
A1B3	450.1100	450.1110	-2.2	C24H20FN3OS2	M+H
A1B4	364.1482	364.1484	-0.5	C21H21N3OS	M+H
A1B5	426.1639	426.1640	-0.2	C26H23N3OS	M+H
A1B7	362.1240	362.1226	3.9	C19H20FNO3S	M+H
A1B8	328.1368	328.1371	-0.9	C19H21NO2S	M+H
A1B10	377.1321	377.1324	-0.8	C22H20N2O2S	M+H
A1B11	412.1492	412.1484	1.9	C25H21N3OS	M+H
A1B12	337.1581	337.1586	-1.5	C17H24N2O3S	M+H
A1B13	504.0729	504.0745	-3.2	C26H22BrN3OS	M+H
A2B3	444.1559	444.1546	2.9	C26H22FN3OS	M+H
A2B4	356.1753	356.1763	-2.8	C23H23N3O	M+H
A2B5	420.2081	420.2076	1.2	C28H25N3O	M+H
A2B7	356.1659	356.1662	-0.8	C21H22FNO3	M+H
A2B8	322.1793	322.1807	-4.3	C21H23NO2	M+H
A2B10	371.1763	371.1760	0.8	C24H22N2O2	M+H
A2B11	406.1918	406.1919	-0.2	C27H23N3O	M+H
A2B13	498.1186	498.1181	1.0	C28H24BrN3O	M+H
A3B2	458.1374	458.1370	0.9	C24H24ClNO6	M+H
A3B3	452.1436	452.1444	-1.8	C24H22FN3O3S	M+H
A3B4	366.1829	366.1818	3.0	C21H23N3O3	M+H
A3B5	428.1965	428.1974	-2.1	C26H25N3O3	M+H
A3B7	364.1557	364.1560	-0.8	C19H22FNO5	M+H
A3B8	330.1696	330.1705	-2.7	C19H23NO4	M+H
A3B10	379.1653	379.1658	-1.3	C22H22N2O4	M+H
A3B11	414.1817	414.1818	-0.2	C25H23N3O3	M+H
A5B5	450.2184	450.2182	0.4	C29H27N3O2	M+H
A5B9	351.2084	351.2073	3.1	C22H26N2O2	M+H
A5B10	401.1862	401.1865	-0.7	C25H24N2O3	M+H
A5B11	436.2023	436.2025	-0.5	C28H25N3O2	M+H
A5B13	528.1279	528.1287	-1.5	C29H26BrN3O2	M+H
A6B1	359.1972	359.1971	0.3	C20H26N2O4	M+H
A6B2	444.1560	444.1578	-4.1	C24H26ClNO5	M+H
A6B3	438.1646	438.1652	-1.4	C24H24FN3O2S	M+H
A6B4	352.2025	352.2025	0.0	C21H25N3O2	M+H
A6B7	350.1765	350.1768	-0.9	C19H24FNO4	M+H
A6B8	316.1913	316.1913	0.0	C19H25NO3	M+H
A6B11	400.2016	400.2025	-2.2	C25H25N3O2	M+H
A6B13	492.1276	492.1287	-2.2	C26H26BrN3O2	M+H

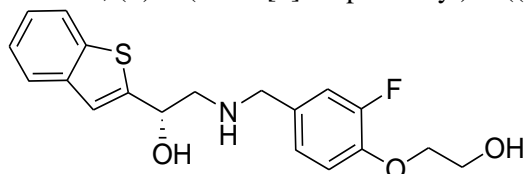
## NMR-spectra of representative $\beta_1$ -receptor matrix compounds

B1-A1B3, (S)-benzyl (2-((2-(benzo[b]thiophen-2-yl)-2-hydroxyethyl)amino)ethyl)carbamate



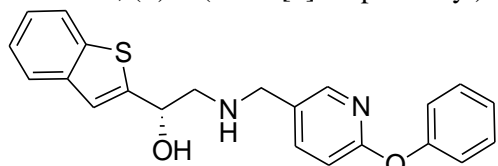
$^1\text{H NMR}$  (500 MHz,  $\text{DMSO-}d_6$ )  $\delta$  8.86 (s; 1H), 7.94 (d;  $J=7.9$ ; 1H), 7.83-7.78 (m; 3H), 7.62 (d;  $J=5.2$  Hz; 1H), 7.55 (d;  $J=3.6$  Hz; 1H), 7.41-7.30 (m; 5H), 7.19 (t;  $J=8.7$  Hz; 1H), 5.45 (dd;  $J=12.9$  Hz; 1H), 4.72-4.66 (m; 1H), 4.43-4.35 (m; 2H), 3.46-3.41 (m; 1H), 3.32-3.26 (m; 1H)

B1-A1B7, (S)-1-(benzo[b]thiophen-2-yl)-2-((3-fluoro-4-(2-hydroxyethoxy)benzyl)amino)ethanol



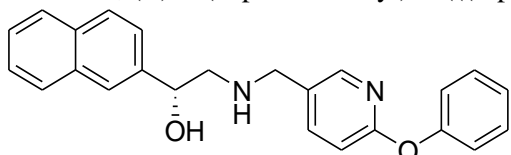
$^1\text{H NMR}$  (500 MHz,  $\text{DMSO-}d_6$ )  $\delta$  7.87 (d;  $J=7.9$  Hz; 1H), 7.74 (d;  $J=7.8$  Hz; 1H), 7.32-7.24 (m; 3H), 7.18 (d;  $J=12.4$ ; 1H), 7.08-7.03(m; 2H), 5.84 (s; 1H), 4.96 (t;  $J=12.6$  Hz; 1H), 4.87 (t;  $J=11.0$  Hz; 2H) 4.02 (t;  $J=10.1$  Hz; 2H), 3.72-3.66 (m; 4H), 2.77 (d;  $J=6.3$  Hz; 2H); 2.06 (s; 1H)

B1-A1B10, (S)-1-(benzo[b]thiophen-2-yl)-2-(((6-phenoxy)pyridin-3-yl)methyl)amino)ethanol



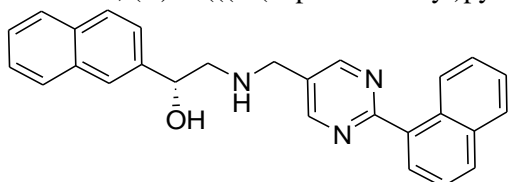
$^1\text{H NMR}$  (500 MHz,  $\text{DMSO-}d_6$ )  $\delta$  8.07 (d;  $J=2.6$  Hz; 1H), 7.88 (d;  $J=7.9$  Hz; 1H), 7.81 (dd;  $J=10.8$  Hz; 1H) 7.74 (d;  $J=8.7$  Hz; 1H), 7.40-7.37 (m; 3H), 7.32-7.25 (m; 3H), 7.19 (t;  $J=14.8$  Hz; m 1H), 7.08 (d;  $J=7.5$  Hz; 2H), 6.95 (d;  $J=8.3$  Hz; 1H), 5.81 (s; 1H), 4.97 (t;  $J=12.4$  Hz; 1H), 3.73 (s; 2H), 2.80-2.78 (m; 2H)

B1-A2B10, (R)-1-(naphthalen-2-yl)-2-(((6-phenoxy)pyridin-3-yl)methyl)amino)ethanol



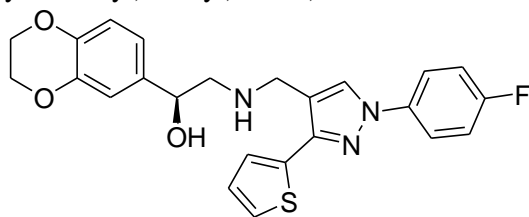
$^1\text{H NMR}$  (500 MHz,  $\text{CDCl}_3$ )  $\delta$  8.09 (d;  $J=2.4$  Hz; 1H), 7.85-7.78 (m; 5H), 7.62 (dd;  $J=10.9$  Hz; 1H), 7.49-7.45 (m; 1H), 7.42 (t;  $J=15.0$  Hz; 2H), 7.22 (t;  $J=14.8$  Hz; 1H), 7.15 (d;  $J=8.5$  Hz; 2H), 6.88 (d;  $J=8.4$  Hz; 1H), 3.65 (t;  $J=12.6$  Hz; 2H), 2.78 (d;  $J=4$  Hz; 1H), 2.72 (d;  $J=6.9$  Hz; 1H) 2.61 (s; 2H), 1.26 (s; 1H)

B1-A2B11, (R)-2-(((2-(naphthalen-1-yl)pyrimidin-5-yl)methyl)amino)-1-(naphthalen-2-yl)ethanol



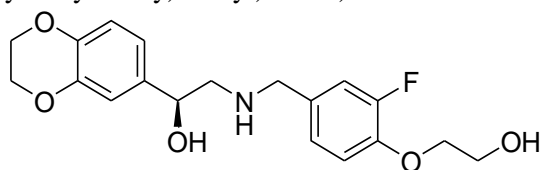
$^1\text{H NMR}$  (500 MHz,  $\text{DMSO-}d_6$ )  $\delta$  8.91 (s; 1H), 8.82 (s; 1H); 8.78 (s; 1H), 8.56-8.52 (m; 1H), 8.04-7.80 (m; 7H), 7.64-7.43 (m; 64.64H), 4.91-4.87 (m; 1H), 4.64 (s; 2H), 3.92 (d;  $J=14.3$ ; 2H), 1.32 (s; 1H)

B1-A3B3, (S)-1-(2,3-dihydrobenzo[b][1,4]dioxin-6-yl)-2-(((1-(4-fluorophenyl)-3-(thiophen-2-yl)-1H-pyrazol-4-yl)methyl)amino)ethanol



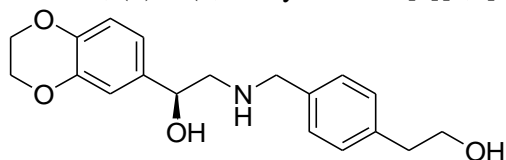
$^1\text{H NMR}$  (500 MHz,  $\text{CDCl}_3$ )  $\delta$  8.12 (s; 1H), 7.68-7.74 (m; 2H), 7.35 (d;  $J=5.0$ ; 2H), 7.13-7.10 (m; 3H), 6.84 (s; 1H), 6.79-6.75 (m; 2H), 4.85 (s; 1H), 4.25-4.16 (m; 7H), 3.04 (d;  $J=44.7$ ; 2H), 1.26 (s; 1H)

B1-A3B7, (S)-1-(2,3-dihydrobenzo[b][1,4]dioxin-6-yl)-2-(((3-fluoro-4-(2-hydroxyethoxy)benzyl)amino)ethanol



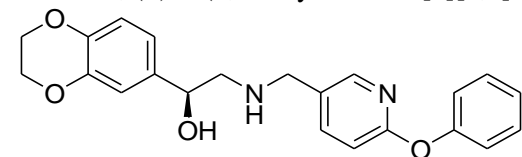
$^1\text{H NMR}$  (500 MHz,  $\text{DMSO-}d_6$ )  $\delta$  7.18 (d;  $J=13.2$  Hz; 1H), 7.19-7.05 (m; 2H), 6.85 (s; 1H), 6.81-6.74 (m; 2H), 4.58 (t;  $J=12.7$  Hz; 1H), 4.20 (s; 1H), 4.18 (s; 4H), 4.03-4.01 (m; 3H), 3.71- 3.69 (m; 4H), 2.59 (d;  $J=7.3$  Hz; 2H), 2.16 (s; 1H)

B1-A3B8, (S)-1-(2,3-dihydrobenzo[b][1,4]dioxin-6-yl)-2-(((4-(2-hydroxyethyl)benzyl)amino)ethanol



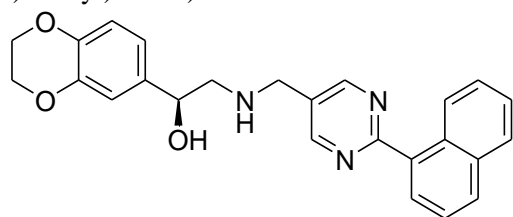
$^1\text{H NMR}$  (500 MHz,  $\text{CDCl}_3$ )  $\delta$  7.26-7.16 (m; 4H), 6.97 (s; 1H), 6.87-6.71 (m; 2H), 4.71-4.65 (m; 1H) 4.24-4.19 (m; 5H), 3.84-3.77 (m; 3H), 2.87-2.81 (m; 4H), 2.59 (s; 2H), 2.27 (s; 1H)

B1-A3B10, (S)-1-(2,3-dihydrobenzo[b][1,4]dioxin-6-yl)-2-(((6-phenoxy-pyridin-3-yl)methyl)amino)ethanol



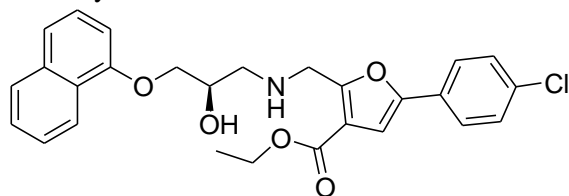
$^1\text{H NMR}$  (500 MHz,  $\text{DMSO-}d_6$ )  $\delta$  8.04 (d;  $J=2.4$  Hz; 1H), 7.78 (dd;  $J=11.0$  Hz; 1H), 7.40 (t;  $J= 15.9$ ; 2H), 7.18 (t;  $J= 13.6$ ; 1H), 7.08 (d;  $J=8.8$  Hz; 2H), 6.95 (d;  $J=8.4$  Hz; 1H), 6.78 (s; 1H), 6.74 (s; 2H), 4.52 (t;  $J=12.4$  Hz; 1H), 4.20-4.16 (m; 5H), 3.68 (s; 2H), 2.56 (d;  $J=7.2$ ; 2H) 2.16 (s; 1H),

B1-A3B11, (S)-1-(2,3-dihydrobenzo[b][1,4]dioxin-6-yl)-2-(((2-(naphthalen-1-yl)pyrimidin-5-yl)methyl)amino)ethanol



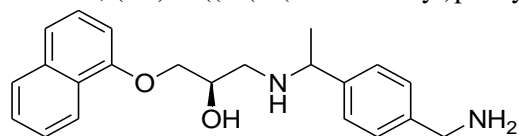
$^1\text{H NMR}$  (500 MHz,  $\text{DMSO-}d_6$ )  $\delta$  8.87 (s; 1H), 8.84 (s; 1H), 8.60 (d;  $J=9.6$  Hz; 1H), 8.03 (d;  $J=7.1$  Hz; 1H), 7.96 (d;  $J=8.1$  Hz; 1H), 7.91 (d;  $J=7.5$  Hz; 1H), 7.85-7.49 (m; 3H), 6.98 (s; 1H), 6.89 (s; 1H), 6.81 (s; 1H), 4.74 (dd;  $J=12.2$  Hz; 1H), 4.69 (s; 1H), 4.21 (s; 4H), 3.90 (s; 2H), 2.93 (dd;  $J=16.0$  Hz; 1H), 2.87-2.83 (m; 1H), 2.27 (s; 1H)

B1-A5B2, (R)-ethyl-5-(4-chlorophenyl)-2-(((2-hydroxy-3-(naphthalen-1-yloxy)propyl)amino)methyl)furan-3-carboxylate



$^1\text{H NMR}$  (500 MHz,  $\text{DMSO-}d_6$ )  $\delta$  8.08 (d;  $J=8.7$  Hz; 1H), 7.86-7.77 (m; 2H), 7.52-7.25 (m; 7H), 6.97 (d;  $J=7.6$  Hz; 1H), 4.41 (t;  $J=10.2$  Hz; 1H), 4.30-4.23 (m; 2H), 2.10-2.03 (m; 2H), 1.90 (d;  $J=11.8$  Hz; 1H), 1.84 (d;  $J=7.0$  Hz; 1H), 1.34-1.23 (m; 3H)

B1-A5B9, (2R)-1-(((1-(4-(aminomethyl)phenyl)ethyl)amino)-3-(naphthalen-1-yloxy)propan-2-ol



$^1\text{H NMR}$  (500 MHz,  $\text{DMSO-}d_6$ )  $\delta$  8.12-8.10 (m; 2H), 8.08 (t;  $J=12.0$  Hz; 2H), 7.90-7.86 (m; 2H), 7.55-7.49 (m; 5H), 7.44 (t;  $J=15.8$  Hz; 1H), 6.96 (d;  $J=6.7$  Hz; 1H), 5.32-5.28 (m; 1H), 4.31 (dd;  $J=14.4$ ; 2H), 4.23-4.20 (m; 3H), 3.59-3.54 (m; 1H), 3.41-3.36 (m; 1H), 2.05 (s; 4H) 1.84 (s; 3H), 1.24 (s; 1H)

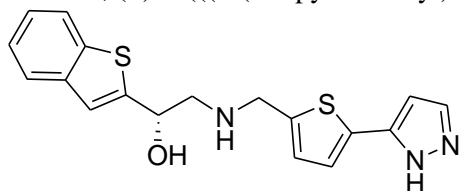
## HR-MS results of the $\beta_2$ -receptor matrix

Compound	Mass (Da)	Calculated Mass (Da)	Measurement Error (ppm)	Formula	Measured Ion
A1B1	333.1018	333.1021	-0.9	C15H16N4O3S	M+H
A1B2	346.1029	346.1032	-0.9	C19H20CINOS	M+H
A1B4	334.0573	334.0572	0.3	C16H15NO3S2	M+H
A1B5	344.0951	344.0957	-1.7	C18H17NO4S	M+H
A1B6	356.0893	356.0891	0.6	C18H17N3OS2	M+H
A1B7	346.0916	346.0913	0.9	C18H16FNO3S	M+H
A1B8	342.1172	342.1164	2.3	C19H19NO3S	M+H
A1B9	370.1037	370.1048	-3.0	C19H19N3OS2	M+H
A1B10	357.0823	357.0828	-1.4	C19H17CIN2OS	M+H
A1B11	386.1422	386.1426	-1.0	C21H23NO4S	M+H
A1B12	388.1218	388.1219	-0.3	C20H21NO5S	M+H
A2B1	327.1443	327.1457	-4.3	C20H19NO4	M+H
A2B2	340.1472	340.1468	1.2	C20H19N3OS	M+H
A2B3	388.1538	388.1549	-2.8	C20H18FNO3	M+H
A2B4	328.1011	328.1007	1.2	C21H21NO3	M+H
A2B5	338.1383	338.1392	-2.7	C21H21N3OS	M+H
A2B6	350.1319	350.1327	-2.3	C21H19CIN2O	M+H
A2B8	336.1595	336.1600	-1.5	C22H23NO5	M+H
A2B10	351.1253	351.1264	-3.1	C19H22CINO3	M+H
A2B11	380.1863	380.1862	0.3	C22H21NO6	M+H
A2B12	382.1649	382.1654	-1.3	C16H17NO5S	M+H
A3B1	335.1356	335.1355	0.3	C19H21N3O3S	M+H
A3B2	348.1371	348.1366	1.4	C19H19CIN2O3	M+H
A3B3	396.1451	396.1447	1.0	C21H25NO6	M+H
A3B4	336.0912	336.0906	1.8	C20H23NO7	M+H
A3B5	346.1296	346.1291	1.4	C18H20N4O4	M+H
A3B6	358.1225	358.1225	0.0	C22H24CINO2	M+H
A3B7	348.1245	348.1247	-0.6	C25H23NO5	M+H
A3B8	344.1489	344.1498	-2.6	C19H19NO4S	M+H
A3B9	372.1393	372.1382	3.0	C21H21NO5	M+H
A3B10	359.1152	359.1162	-2.8	C21H21N3O2S	M+H
A3B12	390.1546	390.1553	-1.8	C22H23NO4	M+H
A5B1	357.1555	357.1563	-2.2	C15H20N4O4	M+H
A5B2	370.1570	370.1574	-1.1	C19H24CINO2	M+H
A5B3	418.1655	418.1654	0.2	C22H23NO5	M+H
A5B4	358.1112	358.1113	-0.3	C16H19NO4S	M+H
A5B5	368.1496	368.1498	-0.5	C18H21NO5	M+H
A5B6	380.1438	380.1433	1.3	C18H21N3O2S	M+H
A5B7	370.1451	370.1455	-1.1	C18H20FNO4	M+H
A5B8	366.1700	366.1705	-1.4	C19H23NO4	M+H
A5B13	460.0758	460.0760	-0.4	C22H22BrNO5	M+H
A5B14	378.1703	378.1705	-0.5	C23H23NO4	M+H
A5B15	425.0857	425.0865	-1.9	C22H21BrN2O2	M+H
A5B16	381.1268	381.1273	-1.3	C21H20N2O3S	M+H
A6B1	321.1559	321.1563	-1.2	C15H20N4O4	M+H
A6B2	334.1564	334.1574	-3.0	C19H24CINO2	M+H
A6B3	382.1646	382.1654	-2.1	C22H23NO5	M+H
A6B4	322.1111	322.1113	-0.6	C16H19NO4S	M+H
A6B5	332.1496	332.1498	-0.6	C18H21NO5	M+H

A6B6	344.1440	344.1433	2.0	C <sub>18</sub> H <sub>21</sub> N <sub>3</sub> O <sub>2</sub> S	M+H
A6B7	334.1451	334.1455	-1.2	C <sub>18</sub> H <sub>20</sub> FNO <sub>4</sub>	M+H
A6B8	330.1708	330.1705	0.9	C <sub>19</sub> H <sub>23</sub> NO <sub>4</sub>	M+H
A6B13	424.0757	424.0760	-0.7	C <sub>19</sub> H <sub>22</sub> BrNO <sub>5</sub>	M+H
A6B14	342.1705	342.1705	0.0	C <sub>20</sub> H <sub>23</sub> NO <sub>4</sub>	M+H
A6B15	389.0861	389.0865	-1.0	C <sub>19</sub> H <sub>21</sub> BrN <sub>2</sub> O <sub>2</sub>	M+H
A6B16	345.1272	345.1273	-0.3	C <sub>18</sub> H <sub>20</sub> N <sub>2</sub> O <sub>3</sub> S	M+H

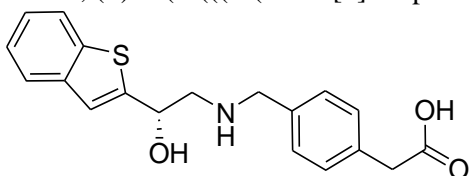
## NMR-spectra of representative $\beta_2$ -receptor matrix compounds

B2-A1B6, (S)-2-(((5-(1H-pyrazol-5-yl)thiophen-2-yl)methyl)amino)-1-(benzo[b]thiophen-2-yl)ethanol



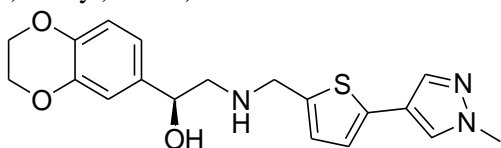
<sup>1</sup>H NMR (500 MHz, DMSO-*d*<sub>6</sub>)  $\delta$  12.73 (s; 1H), 7.88 (d; *J*=8.0 Hz; 1H), 7.74-7.71 (m; 2H), 7.32-7.24 (m; 2H), 7.19-7.16 (m; 1H), 6.91-6.87 (m; 2H), 6.51 (s; 1H), 5.81 (s; 1H), 4.98-4.94 (m; 1H), 3.92 (s; 2H), 2.83 (d; *J*=6.3 Hz; 2H), 1.22 (s; 1H)

B2-A1B8, (S)-2-(4-(((2-(benzo[b]thiophen-2-yl)-2-hydroxyethyl)amino)methyl)phenyl)acetic acid



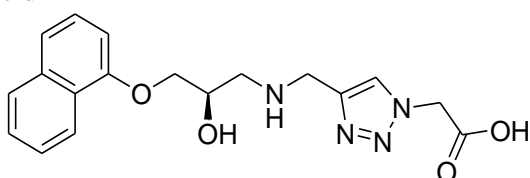
<sup>1</sup>H NMR (500 MHz, DMSO-*d*<sub>6</sub>)  $\delta$  7.89 (d; *J*=7.9 Hz; 1H), 7.75 (d; *J*=7.4 Hz; 1H), 7.45 (d; *J*=8.0 Hz; 1H), 7.34-7.11 (m; 6H), 5.72 (s; 1H), 5.05-5.03 (m; 1H), 3.83 (s; 1H), 3.58-3.49 (m; 4H), 2.88 (d; *J*=4.1 Hz; 1H), 2.73-2.71 (m; 1H), 2.06 (s; 1H)

B2-A3B9, (S)-1-(2,3-dihydrobenzo[b][1,4]dioxin-6-yl)-2-(((5-(1-methyl-1H-pyrazol-4-yl)thiophen-2-yl)methyl)amino)ethanol



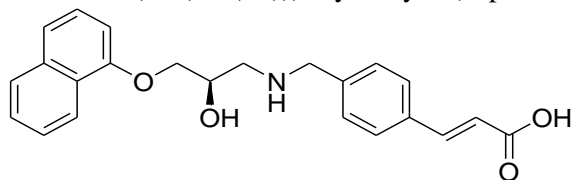
<sup>1</sup>H NMR (500 MHz, DMSO-*d*<sub>6</sub>)  $\delta$  7.91 (s; 1H), 7.61 (s; 1H), 6.93 (d; *J*=3.3 Hz; 1H), 6.81 (d; *J*=3.3 Hz; 1H), 6.77 (s; 1H), 6.74 (s; 2H), 4.52 (t; *J*=12.9 Hz; 1H), 4.19 (s; 1H), 4.17 (s; 4H), 3.84 (s; 2H), 3.81 (s; 3H), 2.61 (t; *J*=13.2 Hz; 2H), 1.22 (s; 1H)

B2-A5B1, (R)-2-(4-(((2-hydroxy-3-(naphthalen-1-yloxy)propyl)amino)methyl)-1H-1,2,3-triazol-1-yl)acetic acid



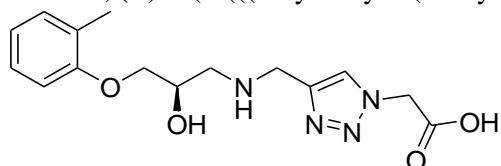
<sup>1</sup>H NMR (500 MHz, DMSO-*d*<sub>6</sub>)  $\delta$  8.21 (d; *J*=7.3 Hz; 1H), 7.84 (d; *J*=9.4 Hz; 1H), 7.74 (s; 1H), 7.51-7.36 (m; 4H), 6.94 (d; *J*=8.1 Hz; 1H), 5.15 (br.s; 1H), 4.58 (s; 2H), 4.13-4.10 (m; 1H), 4.05 (d; *J*=6.4 Hz; 2H), 3.76 (s; 2H), 2.83 (dd; *J*=16.2 Hz, 1H), 2.75 (dd; *J*=18.4 Hz; 1H), 2.06 (s; 1H)

B2-A5B14, (R,E)-3-(4-(((2-hydroxy-3-(naphthalen-1-yloxy)propyl)amino)methyl)phenyl)acrylic acid



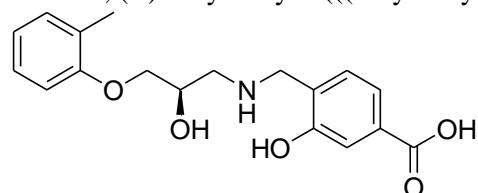
$^1\text{H NMR}$  (500 MHz,  $\text{DMSO-}d_6$ )  $\delta$  8.15 (d;  $J=8.3$  Hz; 1H), 7.84 (d;  $J=8.0$  Hz; 1H), 7.53-7.33 (m; 9H), 6.94 (d;  $J=7.5$  Hz; 1H), 6.43 (d;  $J=15.9$  Hz; 1H), 5.06 (br.s; 1H), 4.14-4.11 (m; 1H), 4.06 (d;  $J=7.0$  Hz; 2H), 3.76 (s; 2H), 2.77 (dd;  $J=16.3$  Hz; 1H), 2.68 (dd;  $J=18.0$  Hz; 1H), 1.22 (s; 1H)

B2-A6B1, (R)-2-(4-(((2-hydroxy-3-(o-tolyloxy)propyl)amino)methyl)-1H-1,2,3-triazol-1-yl)acetic acid



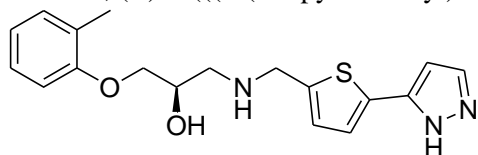
$^1\text{H NMR}$  (500 MHz,  $\text{DMSO-}d_6$ )  $\delta$  7.91 (s; 1H), 7.11 (t;  $J=14.9$  Hz; 2H), 6.89-6.78 (m; 2H), 4.73 (s; 2H), 4.48 (s; 1H), 4.09-4.04 (m; 1H), 3.98 (s; 1H), 3.90 (d;  $J=4.7$  Hz; 2H), 2.98 (dd;  $J=16.0$  Hz; 1H), 2.85- 2.80 (m; 1H), 2.11 (s; 3H); 2.06 (s; 1H)

B2-A6B5, (R)-3-hydroxy-4-(((2-hydroxy-3-(o-tolyloxy)propyl)amino)methyl)benzoic acid



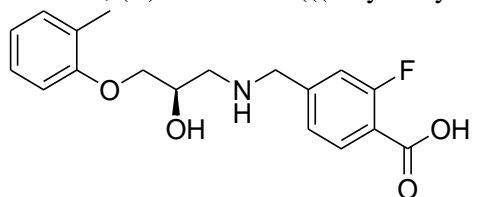
$^1\text{H NMR}$  (500 MHz,  $\text{DMSO-}d_6$ )  $\delta$  7.37 (s; 1H), 7.35-7.32 (m, 2H), 7.29 (d;  $J=8.3$  Hz; 1H), 7.13-7.08 (m; 1H), 6.88 (d;  $J=8.1$  Hz; 1H), 6.82 (t;  $J=14.6$  Hz; 1H), 4.49 (s; 1H), 4.03-4.01 (m; 1H), 3.95 (s; 1H), 3.91 (t;  $J=11.3$  Hz; 2H), 3.15 (s; 2H), 2.87 (dd;  $J=15.9$  Hz; 1H), 2.75 (dd;  $J=19.8$ ; 1H), 2.08 (s; 3H)

B2-A6B6, (R)-1-(((5-(1H-pyrazol-5-yl)thiophen-2-yl)methyl)amino)-3-(o-tolyloxy)propan-2-ol



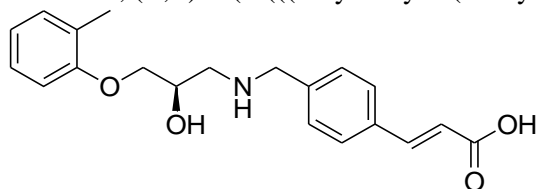
$^1\text{H NMR}$  (500 MHz,  $\text{DMSO-}d_6$ )  $\delta$  12.76 (d;  $J=12.7$  Hz; 1H), 7.71 (s; 1H), 7.17-7.03 (m; 3H), 6.91-6.74 (m; 3H), 6.52 (d;  $J=12.3$  Hz; 1H), 4.03-3.98 (m; 1H), 3.94-3.79 (m; 5H), 2.76 (dd;  $J=15.9$  Hz; 1H), 2.65-2.61 (m; 1H), 2.10 (s; 3H), 2.03 (s; 1H)

B2-A6B7, (R)-2-fluoro-4-(((2-hydroxy-3-(o-tolyloxy)propyl)amino)methyl)benzoic acid



$^1\text{H NMR}$  (500 MHz,  $\text{DMSO-}d_6$ )  $\delta$  7.76 (t;  $J=15.5$  Hz; 1H), 7.25 (d;  $J=20.2$  Hz; 1H), 7.15-7.08 (m; 3H), 6.88 (d;  $J=8.0$  Hz; 1H), 6.81 (t;  $J=14.3$  Hz; 1H), 5.31 (d;  $J=10.0$  Hz; 1H), 3.92-3.88 (m; 4H), 3.80 (a; 1H), 2.71 (d;  $J=11.3$  Hz; 2H), 2.08 (s; 3H), 2.06 (s; 1H)

B2-A6B14, (R,E)-3-(4-(((2-hydroxy-3-(o-tolyloxy)propyl)amino)methyl)phenyl)acrylic acid



$^1\text{H NMR}$  (500 MHz,  $\text{DMSO-}d_6$ )  $\delta$  7.62-7.51 (m; 3H), 7.36 (d;  $J=7.9$  Hz; 1H), 7.28 (t;  $J=17.2$  Hz; 1H), 7.10 (d; 6.2 Hz; 2H), 6.88 (d;  $J=7.9$  Hz; 1H), 6.81 (t;  $J=14.8$  Hz; 1H), 6.47 (d;  $J=15.9$  Hz; 1H), 3.96-3.86 (m; 3H), 3.76 (s; 2H), 2.70-2.68 (m; 1H), 2.61-2.57 (m; 1H), 2.07 (s; 3H), 2.06 (s; 1H)

## Computational details

### Receptor X-ray structure preparation

Docking calculations were performed using FRED with the basal conformation of the human  $\beta_2$ AR in complex with carazolol (PDB: 2RH1) and a model of the human  $\beta_1$ AR also in a basal state, which was downloaded from the GPCRdb (gpcrdb.org). For 2RH1, all ligands, solvent, lipid molecules as well as the T4-lysozyme insertion were removed. Hydrogen atoms were placed and minimized using the HBUILD module in CHARMM (B. R. Brooks, R.

E. Bruccoleri, B. D. Olafson, D. J. States, S. Swaminathan and M. Karplus, J. Comput. Chem., 1983, 4, 187–217.). CHARMM22 atom types and MPEOE partial charges were assigned using the program Witnotp [Novartis Pharma AG, unpublished].

### Selection of the primary-amine-containing OBP fragments

The fragment-like subset of ZINC 23 (www.zinc-docking.org) containing 1'611'889 fragments was used and all fragments featuring a primary amine were extracted using the PINGUI 'Filter your Library' module, leaving 387'707 fragments. We focused on primary-amine-containing OBP fragments, as most adrenergic receptor ligands feature such a protonable moiety and it is also ideally suited for reductive alkylation in order to grow the potential hits. This reaction was already successfully applied in our previous works.

### Selection of the surrogate SBP fragments and enumeration of the virtual library of bitopic (OBP→SBP) compounds

The MolPort building-blocks dataset was downloaded from the MolPort website and contained 305'838 building blocks at that time (January 2017). All aldehyde-containing building blocks were extracted using the PINGUI 'Filter your Library' module. This procedure yielded 12'454 SBP fragments compatible with reductive alkylation, and thus our growing strategy. Ketones were initially discarded, as they would introduce a chiral center in the derivative

products, but a small set of 1394 ketones with one H-bond donor group was added at a later stage of the project in order to increase diversity of the resulting products, thus giving rise to a total of 13'848 SBP fragments. This dataset was further pruned using our chemist-in-the-loop filtering procedure (Figure S17) in order to improve our chances for a high synthesis success rate. In our experience, frequent interactions with the chemist when designing the molecular matrices cannot be given enough importance. The constraints imposed by our chemist were (i) no building blocks containing two functional groups, i.e. two aldehydes or ketones, such that the occurrence of unwanted side products is minimized, (ii) electron-withdrawing groups (EWG) present on the ring close to the aldehyde are preferred, as they should lead to increased reactivity of the aldehyde, (iii) no ortho decoration on the ring close to the aldehyde in order to avoid steric hindrance that might hamper the reaction and (iv) no building blocks with more than one chiral center. Every compatible building block was then converted to the corresponding surrogate by means of a python script written using the rdkit library ([www.rdkit.org](http://www.rdkit.org)) as reported in our previous work. For each of the five core fragments to grow, the derivative products based on reductive alkylation were generated with the aforementioned aldehyde library and the PINGUI 'Create your Virtual Library' module. Those procedures yielded exactly as many surrogates and virtual products as the initial count of compatible reactants (7'893).

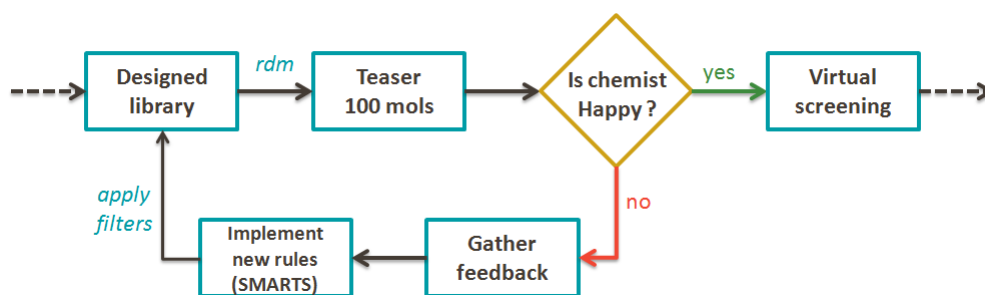


Figure S17: Workflow depicting the CitL (Chemist-in-the-loop) filter aimed at improving the synthesis rate of our matrices.

## Discussion

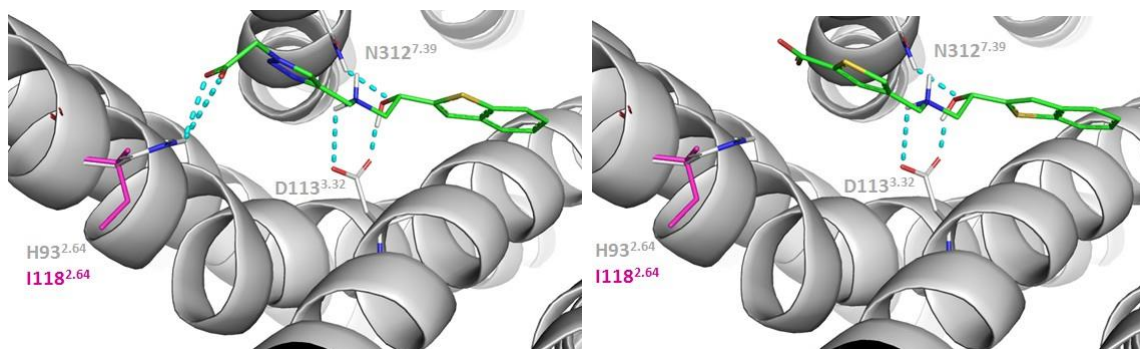


Figure S18: Binding mode prediction of A1B14 (left) and A1B17 (right) in the  $\beta_1$ AR (residues in magenta) and the  $\beta_2$ AR (residues in light grey) binding sites. Ligands are shown with green sticks and polar contacts are represented with cyan dashed lines.

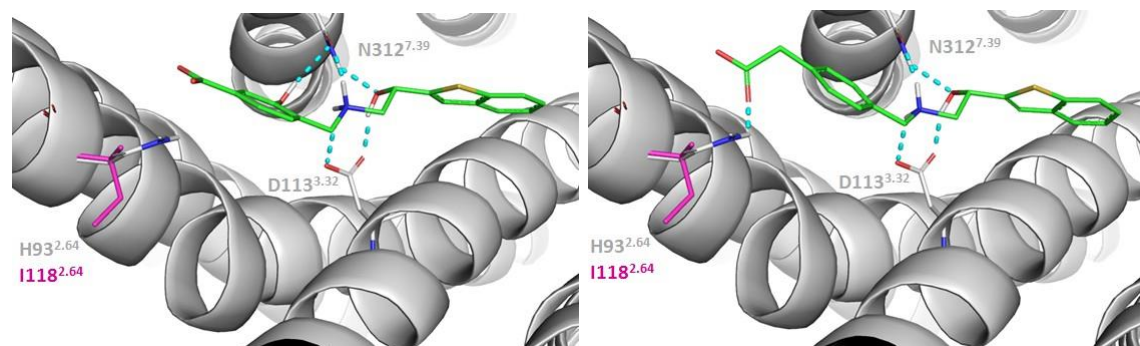


Figure S19: Binding mode prediction of A1B18 (left) and A1B21 (right) in the  $\beta_1$ AR (residues in magenta) and the  $\beta_2$ AR (residues in light grey) binding sites. Ligands are shown with green sticks and polar contacts are represented with cyan dashed lines.